

Using Wavelet Transforms for Hurst Exponent Determination

Ingve Simonsen* and Alex Hansen†

Institutt for fysikk, Norges Teknisk-Naturvitenskapelige Universitet, NTNU, N-7034 Trondheim, Norway

Olav Magnar Nes‡

IKU Petroleum Research, N-7034 Trondheim, Norway

(December 2, 2024)

We propose a new method for Hurst exponent determination based on wavelets. Using this method, we analyze synthetic data with predefined Hurst exponents, fracture surfaces and data from economy. The results are compared to those obtained with Fourier spectral analysis. When many samples are available, the wavelet and Fourier methods are comparable in accuracy. However, when one or only a few samples are available, the wavelet method outperforms the Fourier method with a large margin.

I. INTRODUCTION

It has been known for quite some time that self-affine surfaces are abundant in nature. They can be found in various areas of natural science such as surface growth models [1,2], fractured surfaces [3], geological structures [4], biological systems [5], and even in the mercantile community they have been reported to be seen [6] (and references therein).

Self-affine surfaces in d -dimensional space are described by a set of $d - 1$ roughness exponents. To know these exponents have many important physical implications. First of all, if we know all the roughness exponents, we have full control of the asymptotic statistical properties of the structure. Furthermore, for instance in fracture propagation [3], the exponents are essential in order to determine the universality class of the problem.

It is quite difficult to estimate these exponents from experimental data. Too often statements are made which are based on rather marginal data analysis. It is therefore important to search for alternative ways of analyzing the data — even if the new methods are not better than those already in existence. More tools to analyze the data, widens the possibility to cross-check the conclusions. It is in this spirit that we present in this paper a new method for determining roughness exponents. The strong point of this new method is its excellent averaging properties that makes it possible to extract roughness exponents with high precision even when one or only a few samples are available.

Traditionally, the methods used to determine the self-affine exponents are done in $(1 + 1)$ -dimensions ($d = 2$). In this case we have a single (self-affine) exponent and it is usually referred to as the *Hurst* or roughness exponent. Over the last decade or so, there have been developed several different methods in order to measure this exponent from experimental data (see Ref. [7] and references therein). The most popular method seems to be the *Fourier power spectrum method* (FPS) and we will use this method as a “reference” here. A systematic study of the quality of this and other traditional methods is found in Ref. [7].

The wavelet transform is an integral transform developed in the early eighties in signal analysis and is today used in different fields ranging from quantum physics and cosmology to data compression technology. Since the late eighties, wavelets has been an active research field in pure and applied mathematics, and large theoretical progress has been made. The wavelet transform behaves as a mathematical microscope which decomposes an input signal into amplitudes which depend on position and scale. For this purpose localized functions, called wavelets, are being used. By changing the scale of the wavelet, one is able at a certain location to focus on details at higher and higher resolution. By taking advantage of the central properties of self-affine functions, we derive a scaling relation between wavelet amplitudes at different scales, from which the Hurst exponent can be extracted. The method is easily generalized to higher dimensions.

*Ingve.Simonsen@phys.ntnu.no

†Alex.Hansen@phys.ntnu.no

‡Olav-Magnar.Nes@iku.sintef.no

To our knowledge, two papers discuss wavelet based techniques in connection with Hurst exponent measurements [8,9]. In [8], the wavelet transform modulus maxima method is introduced, and in [9], wavelet packet analysis is used to extract the Hurst exponent. The method we present here differ from both of these.

This paper is organized as follows. In Sec. II we review the central properties of self-affine surfaces, while in Sec. III the wavelet transform is reviewed. Sec. IV presents the derivation of the scaling relation for self-affine functions in the wavelet domain. In Sec. V this scaling relation is applied to synthetic and experimental data, and Hurst exponents are extracted. Finally, in Sec. VI, our conclusion is presented.

II. SELF AFFINE SURFACES

As mentioned in the introduction, self-affine surfaces, which are generalizations of Brownian motion [10,11], have statistical properties characterized by a set of exponents. Let us assume that we have a function, $h(x)$, of one variable only (for simplicity), i.e., a fractional Brownian motion [10,11]. Here x is the horizontal variable, while h is the vertical one. The self affinity is defined through statistical invariance under the transformation

$$x \rightarrow \lambda x, \tag{1a}$$

$$h \rightarrow \lambda^H h. \tag{1b}$$

Here H is the Hurst exponent. By combining such transformations, one can construct the affine group. Thus, self-affine surfaces are (statistically) invariant under the affine group. An alternative way of expressing this invariance is by

$$h(x) \simeq \lambda^{-H} h(\lambda x). \tag{2}$$

Here the symbol \simeq means statistical equality. This form will prove useful later. The Hurst exponent, H , is limited to the range $0 \leq H \leq 1$. The lower limit comes along by requiring the surface width to decrease when smaller sections of the surface is studied (the opposite being unphysical), while the upper limit comes from assuming the surface to be asymptotically flat.

Eqs. (1) and (2) express that for self-affine functions one must rescale the horizontal and vertical direction differently in order to have statistical invariance. Thus, self-affine surfaces are by construction anisotropic in the horizontal and vertical direction, except when $H = 1$ (self-similarity). The Hurst exponent, H , expresses the tendency for $dh = \frac{dh(x)}{dx} dx$ to change sign. When $H = 1/2$ (Brownian motion), the sign of dh changes randomly, and the corresponding surface possesses no spatial correlations. When $1/2 < H \leq 1$, the sign tends not to change, while for $0 \leq H < 1/2$, there is a tendency for the sign to change (anti-correlation). In both intervals there are long-range correlations falling off as a power law. Surfaces with $H > 1/2$ are said to be persistent, and those with $H < 1/2$ are anti-persistent.

III. THE WAVELET TRANSFORM

Here we will review some of the important properties of wavelets, without any attempt at being complete. Rather, our aim is to provide enough background for the discussion that follows. For a more complete treatment of wavelets, see e.g. Ref. [12].

In physics and mathematics there are many examples of problems which are more easily solved in a new set of coordinates (basis), where the Fourier transform being the most famous one. Such transforms consist in calculating the amplitudes for each basis function of the new domain. As long as a set of functions is complete, it can be used as a root for an integral transform.

The wavelet transform is a relatively new (integral) transform. What makes this transform special is that the set of basis functions, known as wavelets, can be chosen to be well-localized (have compact support) both in space and frequency. Thus, one has some kind of “dual-localization” of the wavelets. This contrasts the situation met for the Fourier Transform where one only has “mono-localization”, meaning that localization in both position and frequency simultaneously is not possible.

The wavelets are parameterized by a *scale parameter* (dilation parameter) $a > 0$, and a *translation parameter* $-\infty < b < \infty$. What makes the wavelet transform remarkable is that the wavelet basis can be constructed from one single function $\psi(x)$ according to

$$\psi_{a;b}(x) = \psi\left(\frac{x-b}{a}\right). \quad (3)$$

In usual terminology, $\psi(x)$ is the mother function or *analyzing wavelet*.

Given a function $h(x)$, the (continuous) wavelet transform is defined as

$$\mathcal{W}[h](a, b) = \frac{1}{\sqrt{a}} \int_{-\infty}^{\infty} \psi_{a;b}^{\dagger}(x) h(x) dx \quad (4)$$

Here $\psi^{\dagger}(x)$ denotes the complex conjugate of $\psi(x)$. We should emphasize that some authors use a somewhat different definition when it comes to the prefactor. The specific formulas we derive further on in analyzing the self-affine surfaces depends on the definition we have chosen.

In order for a function $\psi(x)$ to be usable as an analyzing wavelet, one must demand that it has zero mean. However, in nearly all applications it is in addition required to be orthogonal to some lower order polynomials, i.e.,

$$\int_{-\infty}^{\infty} x^m \psi(x) dx = 0, \quad 0 \leq m \leq n. \quad (5)$$

Here the upper limit n is related to what is called the order of the wavelet. The larger n the higher order has the wavelet the smoother it is.

Unlike for instance the more familiar Fourier transform, the wavelet transform is not completely specified before the analyzing wavelet (i.e., the basis) is given. There is a large number of possible candidates, but we will concentrate exclusively on one of the most popular families, namely the Daubechies wavelet family [12].

In order for the wavelet transform to be useful for numerical calculations, it has to be accompanied by an effective numerical implementation. Such an algorithm was developed by Mallat, and the resulting transform is known as the discrete wavelet transform [13].

IV. THE AVERAGED WAVELET COEFFICIENT METHOD

As was shown in Sec. II, the defining feature of self-affine profiles is the scaling property (cf. Eqs. (1) and (2)). According to Eq. (2) one should have $\mathcal{W}[h(x)](a, b) \simeq \mathcal{W}[\lambda^{-H} h(\lambda x)](a, b)$ for a self-affine function $h(x)$ in the wavelet domain. Here, in expressions like $\mathcal{W}[h(x)](a, b)$, we have included the x -dependence explicitly for convenience.

Hence after a simple change of variable one has:

$$\begin{aligned} \mathcal{W}[h(x)](a, b) &\simeq \mathcal{W}[\lambda^{-H} h(\lambda x)](a, b) \\ &= \frac{1}{\sqrt{a}} \int_{-\infty}^{\infty} \lambda^{-H} h(\lambda x) \psi^{\dagger}\left(\frac{x-b}{a}\right) dx \\ &= \lambda^{-\frac{1}{2}-H} \frac{1}{\sqrt{\lambda a}} \int_{-\infty}^{\infty} h(x') \psi^{\dagger}\left(\frac{x' - \lambda b}{\lambda a}\right) dx' \\ &= \lambda^{-\frac{1}{2}-H} \mathcal{W}[h(x)](\lambda a, \lambda b). \end{aligned}$$

Thus, we have

$$\mathcal{W}[h](\lambda a, \lambda b) \simeq \lambda^{\frac{1}{2}+H} \mathcal{W}[h](a, b). \quad (6)$$

Note that this scaling relation relies heavily on the definition (4), so for other definitions of the wavelet transform, this equation must be changed accordingly. What the scaling relation (6) expresses, is that if we perform an (isotropic) rescaling (with factor λ) of the wavelet domain of a self-affine function, this is the same as rescaling the wavelet amplitude of the original domain with a factor $\lambda^{\frac{1}{2}+H}$.

From the definition of the wavelet transform, it follows directly that the wavelet domain of a one-dimensional function is two-dimensional; one dimension corresponding to scale and the other to space (translation). So, for instance for a specified scale, we have an infinite number of amplitudes corresponding to various translation parameters b . When one is analyzing self-affine functions, like any fractal, it is the scale rather than the translation which is of general interest to us. With this in mind, we propose to *average out* the dependency on the translation parameter in the wavelet domain in order to find a representative amplitude at a given scale. We suggest to use the following formula for the average

$$W[h](a) = \langle |\mathcal{W}[h](a, b)| \rangle_b, \quad (7)$$

where $\langle \cdot \rangle_b$ is the standard arithmetic mean value operator with respect to the variable b . Hence the scaling relation (6) becomes

$$W[h](\lambda a) \simeq \lambda^{\frac{1}{2}+H} W[h](a). \quad (8)$$

The strategy for the data-analysis should now be clear: (1) Wavelet transform the data into the wavelet domain. (2) Calculate the averaged wavelet coefficient $W[h](a)$ according to Eq. (7). (3) Plot $W[h](a)$ against scale a in a log-log plot. A scaling regime consisting of a straight line in this plot implies a self-affine behavior of the data. The slope of this straight line is $\frac{1}{2} + H$.

We call this method the *Averaged Wavelet Coefficient* (AWC) method.

V. DATA ANALYZES WITH THE AVERAGED WAVELET COEFFICIENT (AWC) METHOD

A. Synthetic data

We are now in position to test our scaling relation (8) on artificial and real data, and estimate the corresponding Hurst exponents. We start by performing an AWC-analysis on a set of artificially generated self-affine profiles with predefined Hurst exponents. The self-affine generator used in this work is the Voss algorithm [14], which also is known as the (iterated) midpoint displacement algorithm. The quality of a given analyzing method is assessed by the difference between the Hurst exponent chosen for the Voss-generator, and the estimated value from the analysis.

In our first illustration of the practical performance of the AWC method, we have generated $N = 100$ artificial profiles with Hurst exponent $H = 0.7$ and length $L = 4096$. The wavelet used here and from now on if nothing different is indicated, is the Daubechies wavelet of order 12 (Daub12). We will later demonstrate that this choice of wavelet order is not crucial in any way. For each sample the mean drift of the profile, defined as the line connecting its first and last point, is subtracted. In Fig. 1 the results are presented for both the AWC- and Fourier power spectrum (FPS) density method. In both cases a straight line fit is performed to the (log-log) data, with resulting slopes of respectively 1.19 ± 0.01 and -2.39 ± 0.02 . Theoretically these slopes should be $\frac{1}{2} + H$ (cf. Eq. (8)) and $-(1 + 2H)$ [10,11] for respectively the AWC- and FPS-method. Hence the corresponding estimated Hurst exponents, in obvious notation, become $H_W = 0.69 \pm 0.01$ and $H_F = 0.70 \pm 0.01$. Here we should emphasize that the errors indicated, are only the regression errors in the actual region. Errors due to different choices of regression regions are not included even if they typically are larger than the regression error itself. The quality of the fit is indicated in Figs. 1a and 1c, by including the fitting function. Empirically we would expect the *total* error of the Fourier power spectral density method to be larger than the corresponding error of the AWC method. This is so because the linear scaling region is smallest for the FPS-method. In order to quantify the behavior for different Hurst exponents, we have performed a corresponding analysis to the above, for various exponents in the range $0 < H < 1$. The results are shown in Figs. 1c and 1d. We observe that there are good agreement between the actual and estimated exponents in the whole range of Hurst exponents independent of method.

It is often the case that one does not have many data samples available for analysis, especially when dealing with experimental data. To discuss this situation we have performed the same analysis as above, but now with a smaller number of samples (see Figs. 2 and 3). Still the correspondence with the input value is relatively good. However, for small number of samples the uncertainty in the slope determination becomes large, as illustrated in Figs. 3a and 3c. This tendency is much more explicit for the FPS-method than for the AWC-approach.

One could now ask how these results depend on the specific order chosen for actual wavelet. In Fig. 4 we have included a graph showing the AWC-function, $W[h](a)$, for different orders (i.e. smoothness) of the Daubechies wavelet family. With the above comment made on the true error in the Hurst exponent measurements, we conclude that within the actual errors the AWC method does not seem to be sensitive to the order of the wavelet, at least not for the Daubechies wavelet family. A non-systematic study with other kind of wavelets does not seem to change this conclusion.

We have also investigated the situation where the length of the profiles varies. Our findings are compiled in Table I. The results are generally in agreement with the input value for system sizes larger or equal to $L = 256$. It should also be noted that the regression error (not necessarily the actual error) generally decreases with increasing system size. This is as expected because when the system size increases the scaling region becomes larger, resulting in a better regression fit.

In summary, for the study of (clean) synthetic self-affine data, we may conclude that the AWC method works well. It is in particular a good choice when only a few number of samples are available which is often the case in many experimental situations.

B. Stability against noise and distortions

All real measurements are subject to noise and distortions. These may have their origin in measuring uncertainties, instrumental noise and non-linearities that might transform the signal in some way. The non-linearities may come from the response of the measuring devices used. However, it may also be that the variable studied is not the “good” one. In order for an method of analysis to be useful for real world data, it has to be stable with respect both to noise and to distortions.

We start by studying distortions. Suppose that rather than measuring the *generic* self-affine function $h(x)$, we observe $F[h(x)]$, i.e.,

$$h(x) \rightarrow F[h(x)], \quad (9)$$

which is a one-to-one transformation. Note that we have not allowed for an explicit x -dependence in F , because this may destroy the self-affinity (more about this later). By other methods it can be demonstrated that the transformation (9) does not change the Hurst exponent [4]. A qualitative to understand this result is that, since the Hurst exponent H is related to the tendency of dh to change sign (see earlier discussion), the Hurst exponent should be insensitive to transformations of the type (9) as long as F is a relatively smooth functional. To demonstrate the stability of the AWC method to such distortions, we have performed a numerical experiment, where we have put $F[h(x)] = \log_{10}(h(x))$, and then calculated the Hurst exponent from $F[h(x)]$. The result is shown in Fig. 5, and as can be seen, the Hurst exponent is unchanged within the numerical errors.

It is easy to see that if the functional F has some explicit dependence on the “horizontal” coordinate (i.e. x in our case), the self-affine correlation property may be destroyed. Spatial noise of any kind, has exactly this property. Since such noise is usually always found in real data, it is important to investigate how sensitive the AWC-algorithm is to such artefacts. In order to simulate this situation, we apply the functional $F[h(x)] = h(x) + \eta(x)$, where $\eta(x)$ is a noise term, to clean self-affine data $h(x)$, and then proceed with the AWC analysis. The amount of noise added to the data, i.e., the noise rate χ , is defined as $\chi = \frac{\max|\eta(x)| - \min|\eta(x)|}{\max|h(x)| - \min|h(x)|}$.

In this paper we have chosen to work with white and pink (i.e., $1/f$) noise. Quite recently Aguilar and coworkers have pointed out that scanning tunneling microscopy instrument noise is pink [15]. The results for the case $\chi = 10\%$ of added white or pink noise are shown in Fig. 6. In both cases we see that the AWC method extracts the actual Hurst exponent quite well. Notice that for the white noise case, only the lower scales seem to be considerably affected by the noise, and a nice cross-over to the (now smaller) scaling regime is shown. However, for the pink noise the whole region is affected without introducing significant changes over the non-noisy results. We have also investigated the case of a noise rate of $\chi = 25\%$ (results not shown), with the result that it was not possible to extract the Hurst exponent with any level of confidence.

Self-affine scaling behavior is usually only found over a limited region of space (or time), and it is important to be able to estimate these cross-over scales. To be able to investigate the potential of the AWC method in this respect, we have generated some artificial self-affine profiles with $H = 0.7$ and length $L = 4096$ and used a standard 5-point filter to destroy the self-affine correlations at small distances (i.e. destroy correlations between 11 subsequent points). For the AWC method we should expect to see a cross-over at scales $a_c = \frac{11}{4096} \simeq 0.003$, while for the FPS-method the cross-over frequency is expected at $f_c = 0.09$. As can be seen from Fig. 7, this is indeed what we find. For the largest number of sample ($N = 100$) the AWC and FPS method are equivalent, but for only one sample the cross-over is most easily seen for the wavelet method as shown in Figs. 7c and d.

C. Real data

As mentioned in the introduction, self-affine surfaces can be found many places in natural and non-natural sciences. Here we will in particular discuss two quite different examples, clearly demonstrating the general presence of self-affine structures.

Our first example is taken from natural science, and concerns the structure of a fractured granite surface [16]. It contains 2050×211 data points. One representative profile of this surface is given in Fig. 8a. The results of the

wavelet and Fourier analysis, using the methods described earlier in this paper, are collected in Figs. 8b and c . We see that there are nice scaling regions in both cases indicating that the fractured granite surface is indeed self-affine. The Hurst exponents, obtained by a regression fit to the scaling region, are $H_W = 0.81 \pm 0.02$ and $H_F = 0.79 \pm 0.03$ respectively for the AWC and FPS method. Note that also here only the regression error is indicated and that the “true error” is somewhat larger. The results for the two methods are consistent and coincide with the results of other studies of fracture granite surfaces [17]. We would like to emphasize that the reason for the good agreement between the two methods, and the good quality of both regression fits are due mainly to the large number of samples available. It is interesting to observe that the exponent for the fractured granite surface reported here, is in complete agreement with earlier speculations that fractured surfaces should have a universal Hurst exponent of $H = 0.8$ [3,18,19]

Unfortunately, the availability of large number of samples is notoriously not always the case, nor is it appropriate to talk about several samples at all in some situations. In order to illustrate this point, we have included share prices for the Italian automobile manufacturer FIAT taken from the Milan Stock Exchange for the period from the 2nd of January 1985 to the 4th of May 1992 with three quotes per day [20] (Figs. 9a and b). Observe that in this case, it is not relevant to talk about samples for a specified period of time; only one sample for a given time period is available. Since the Fiat data contains an “upward” trend throughout the year of 1985 (see Fig. 9a), the whole data set is not well suited for a self-affine analysis. Instead, we have chosen a portion of the initial data, indicated as a window in Fig. 9a, and shown in Fig. 9b. The time period of this window starts at the 1st of September 1988 and ends at the 28th of May 1991. The result of the corresponding analysis is given in Figs. 9c and d. The estimated Hurst exponents are $H_W = 0.65 \pm 0.03$ from the AWC method while the FPS method gives $H_F = 0.62 \pm 0.06$. These two results are consistent, but there are noticeable difference in the accuracy of the regression fits for the two methods. This is most easily seen by comparing Figs. 9c and d by visual inspection. The error bars associated with the FPS analysis, based solely on the regression analysis, are in particular underestimated. It is difficult to identify a scaling region at all. We find it very interesting to observe that a Hurst exponent $H = 0.65$ is observed in the stock marked simulations by Bak et al. [6] when using the Urn model with volatility feedback.

This example, is in our view, a very good example of the power of the AWC method in cases where few samples are available, and we believe it to have potential of becoming a useful method in practical situations.

VI. CONCLUSIONS

We have introduced, derived and tested a new simple method for Hurst exponent measurements based on the wavelet transform. It has been compared to the Fourier power spectrum method where appropriate. We find that the two methods performs approximately equally for large number of samples. However, for lower numbers of samples this new method outperforms the more traditional Fourier transform based method. The AWC method are also demonstrated to handle noisy and experimental data in a satisfactory manner.

ACKNOWLEDGMENTS

We are grateful to J. Schmittbuhl for permission to use his measurements for the fractured granite surface. We also thank B. Vidakovic for providing the Fiat share price data to us. One of the authors (I. S.) thanks the Research Council of Norway and Norsk Hydro AS for financial support. This work has received support from the Research Council of Norway (Program for Supercomputing) through a grant of computing time.

-
- [1] P. Meakin, Phys. Rep. **235**, 189 (1993).
 - [2] L. Barabasi and H. E. Stanley, *Fractal Growth Models* (Cambridge University Press, Cambridge, 1995).
 - [3] E. Bouchaud, G. Lapasset and J. Planès, Europhys. Lett, **13**, 73 (1990).
 - [4] A. Hansen and O. M. Nes, *IKU Report*, unpublished, 1997.
 - [5] T. Vicsek, M. Cserző and V. K. Horváth, Physica A **167**, 315 (1990).
 - [6] P. Bak, M. Paczuski and M. Shubik, cond-mat/9609144, 1996.
 - [7] J. Schmittbuhl, J. P. Vilotte, and S. Roux, Phys. Rev. E **51**, 131 (1995).
 - [8] A. Arneodo, E. Bacry and J. F. Muzy, Physica A **213**, 232 (1995).

- [9] C. J. Jones, G. T. Loneragan and D. E. Mainwaring, *J. Phys. A* **29**, 2509 (1996).
- [10] J. Feder, *Fractals* (Plenum, New York, 1988).
- [11] K. Falconer, *Fractal geometry: mathematical foundations and application* (John Wiley, Chichester, 1990).
- [12] I. Daubechies, *Ten Lectures on Wavelets* (SIAM, Philadelphia, 1992).
- [13] W. H. Press, S. A. Teukolsky, W. T. Vetterling and B. P. Flannery, *Numerical Recipes*, 2nd edition (Cambridge University Press, Cambridge, 1992).
- [14] R.F. Voss, *Scaling phenomena in disordered Systems* (Plenum, New York, 1985).
- [15] M. Aguilar, E. Anguiano, F. Vazquez and M. Pancorbo, *J. Microscopy* **167**, 197 (1992).
- [16] J. Schmittbuhl, unpublished (1997).
- [17] J. Schmittbuhl, S. Roux and Y. Berthaud, *Europhys. Lett.* **28**, 585 (1994).
- [18] K. J. Måløy, A. Hansen, E. L. Hinrichsen and S. Roux, *Phys. Rev. Lett.* **68**, 213 (1992).
- [19] E. Bouchaud, G. Lapasset, J. Planès and S. Navéos, *Phys. Rev. B* **48**, 2917 (1993).
- [20] Data from B. Vidakovic, <http://www.isds.duke.edu/~brani/datapro.html>.

L	H_W
64	0.67 ± 0.05
128	0.66 ± 0.03
256	0.69 ± 0.02
512	0.70 ± 0.02
1024	0.70 ± 0.01
2048	0.70 ± 0.01
4096	0.70 ± 0.01

TABLE I. Estimated Hurst exponents for the AWC method (H_W) for different system sizes, L . The predefined Hurst exponent was $H = 0.7$, and in all calculations the number of samples used was $N = 100$. The wavelet used was Daub12.

FIG. 1. Hurst exponents estimated by (a and b) the averaged wavelet method (H_W) and (c and d) the Fourier power spectrum density method (H_F). (a) The AWC-function $W[h](a)$ vs scale a for Hurst exponent $H = 0.7$. The solid line is the regression line to the scaling region. The estimated Hurst exponent is $H_W = 0.69 \pm 0.01$. (b) Wavelet estimated Hurst exponents (H_W) for various actual Hurst exponents H . (c) The power spectrum, $P(f)$ vs frequency f for actual Hurst exponent $H = 0.7$. The solid line is the regression fit. The estimated Hurst exponent is $H_F = 0.70 \pm 0.01$. (d) Fourier estimated Hurst exponents (H_F) for various actual Hurst exponents H . The number of samples per data point was $N = 100$. The same profiles were used for both the wavelet and Fourier analysis.

FIG. 2. The same as Fig. 1b and d, but now with the following number of samples $N = 50$ (a and b) and $N = 5$ (c and d).

FIG. 3. The same as Fig. 1, but now with only one sample, $N = 1$.

FIG. 4. The AWC-function $W[h](a)$ vs scale a , for various choices of wavelet order (Daubechies family) as indicated in the figure. The data are for self-affine profiles with Hurst exponent $H = 0.7$, and the number of samples used was $N = 100$.

FIG. 5. (a) The AWC-function $W[g](a)$ vs scale a where $g(x) = \log_{10}(h(x))$ and $h(x)$ is a self-affine function with $H = 0.7$. The number of samples used was $N = 100$. The solid line is the regression fit to the data, and the estimated Hurst exponent was $H_W = 0.70 \pm 0.01$ (b) Wavelet measured Hurst exponents, H_W , for various actual exponents in the range $0.1 \leq H \leq 0.9$.

FIG. 6. The same as Figs. 1a and b, but now with $\chi = 10\%$ white (a and b) or pink (c and d) noise added to the data. The Hurst exponent of the self-affine component of the data in (a) and (c) was $H = 0.7$. The number of samples was $N = 100$. The estimated Hurst exponents for the white and pink case shown in Figs. a and c were respectively $H_W = 0.71 \pm 0.02$ and $H_W = 0.69 \pm 0.01$.

FIG. 7. The wavelet (Figs. a and c) and Fourier (Figs. b and d) analysis of synthetic data with Hurst exponent $H = 0.7$ after applying a 5-point filter to the them. In Figs. a and b, the results are being averaged over $N = 100$ samples, while in Figs. c and d only one single sample ($N = 1$) is being used. The solid lines are the regression fits to the scaling regions. The cross-overs are clearly seen in all cases. Theoretically the cross-over values are $a_c = 0.003$ and $f_c = 0.09$ for the wavelet and Fourier method respectively.

FIG. 8. (a) One single representative profile from the granite fracture. (b) AWC analysis of the granite data. The solid line is the regression fit to the scaling region. The corresponding Hurst exponent is $H_W = 0.81 \pm 0.02$. (c) FPS analysis of the data. Here the solid line corresponds to a Hurst exponent $H_F = 0.79 \pm 0.03$.

FIG. 9. (a) Fiat share prices taken from the Milan Stock Exchange for the period from the 2nd of January 1985 (day 1) to the 4th of May 1992. (b) A detailed view of the square window indicated in (a). The period corresponds to the 1st of September 1988 to the 28th of May 1991. (c) The result of the wavelet analysis for the data in (b). The estimated Hurst exponent, corresponding to the solid line, was $H_W = 0.65 \pm 0.03$. (d) The result of the Fourier analysis for the data in (b). The Hurst exponent in this case was $H_F = 0.62 \pm 0.06$ Note the more well behaved scaling region for the wavelet-method as compared to the Fourier-method.

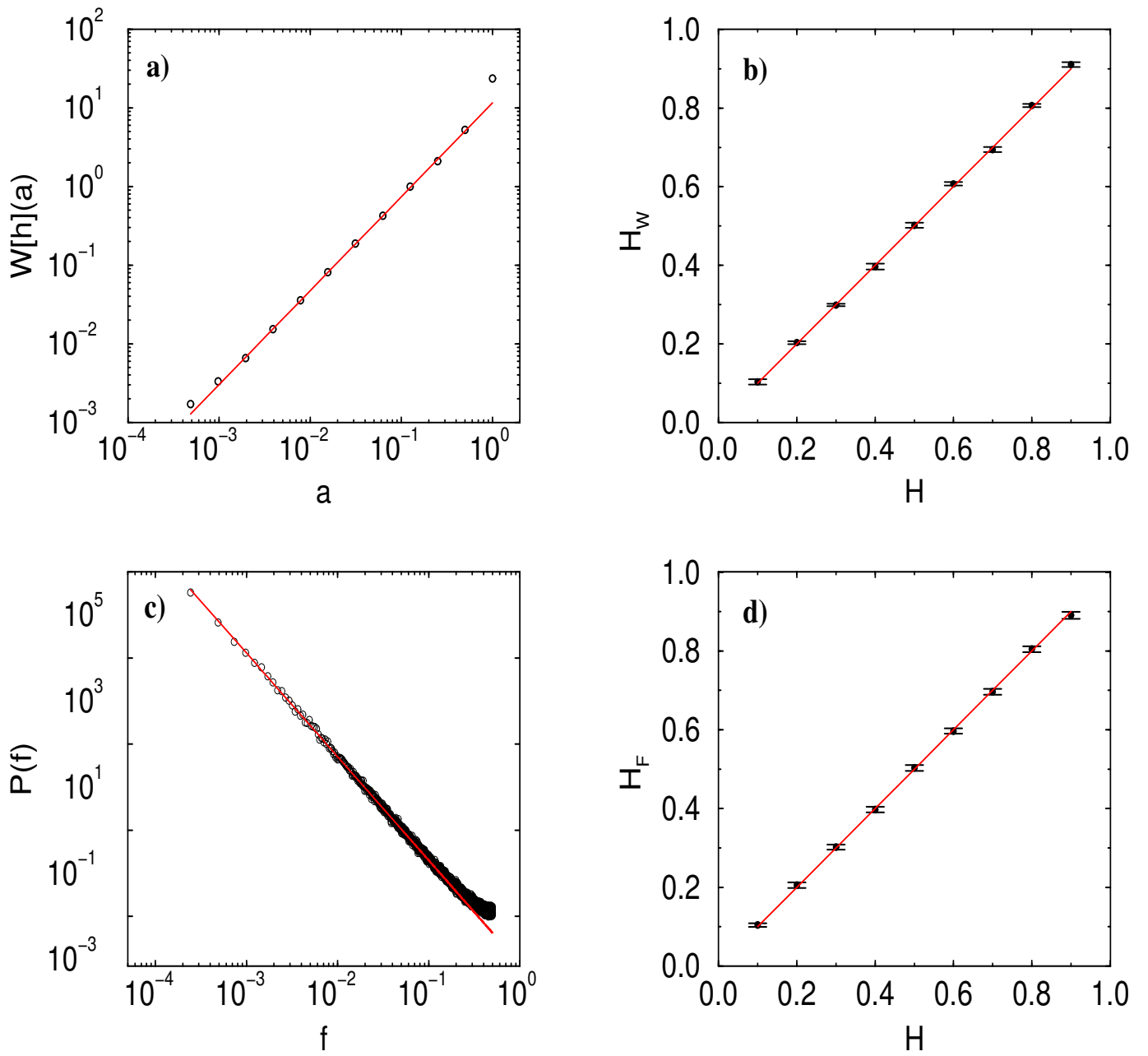


Figure 1

Simonsen, Hansen and Nes

Using the Wavelet transform for Hurst exponent determination

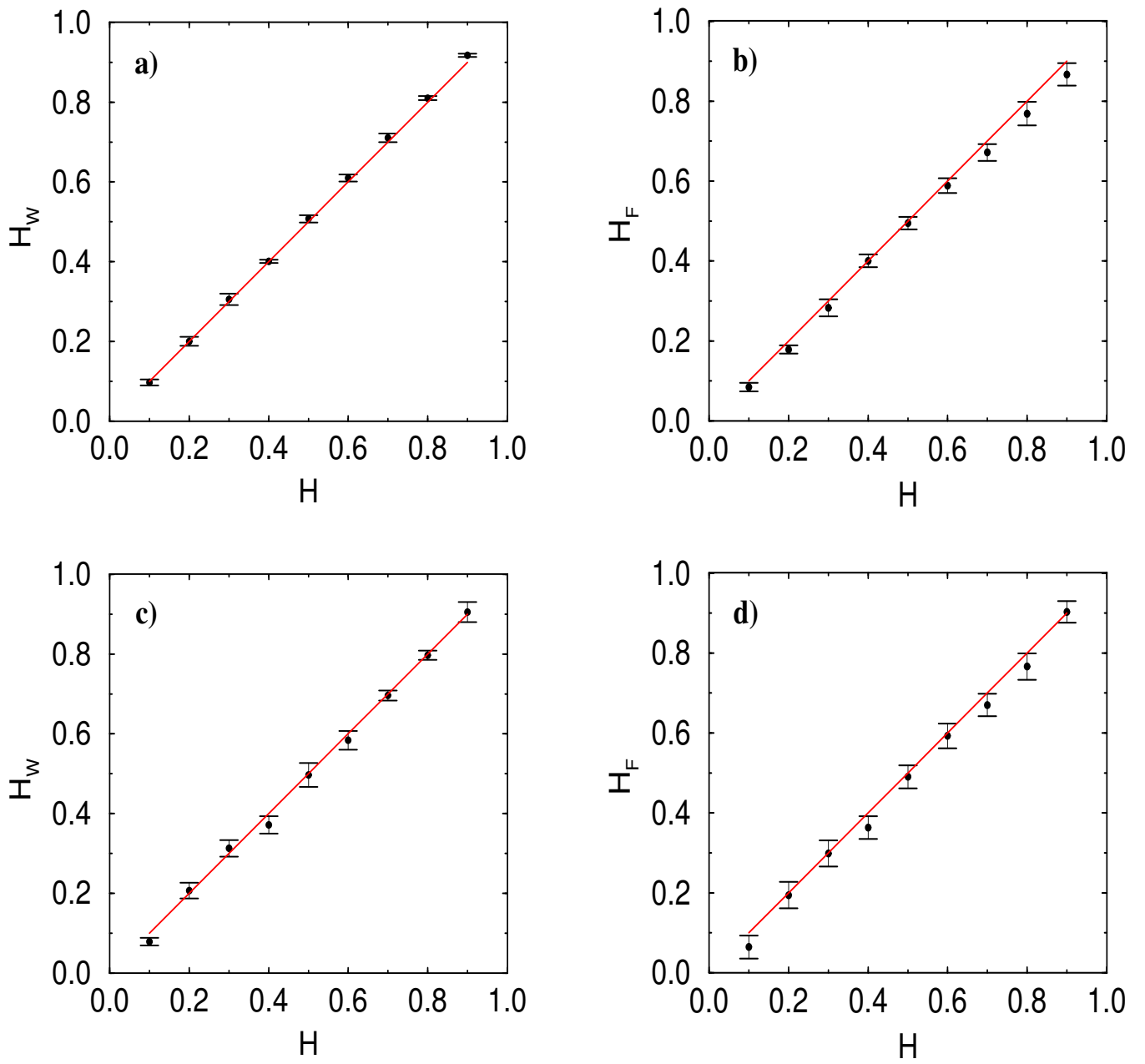


Figure 2

Simonsen, Hansen and Nes

Using the Wavelet transform for Hurst exponent determination

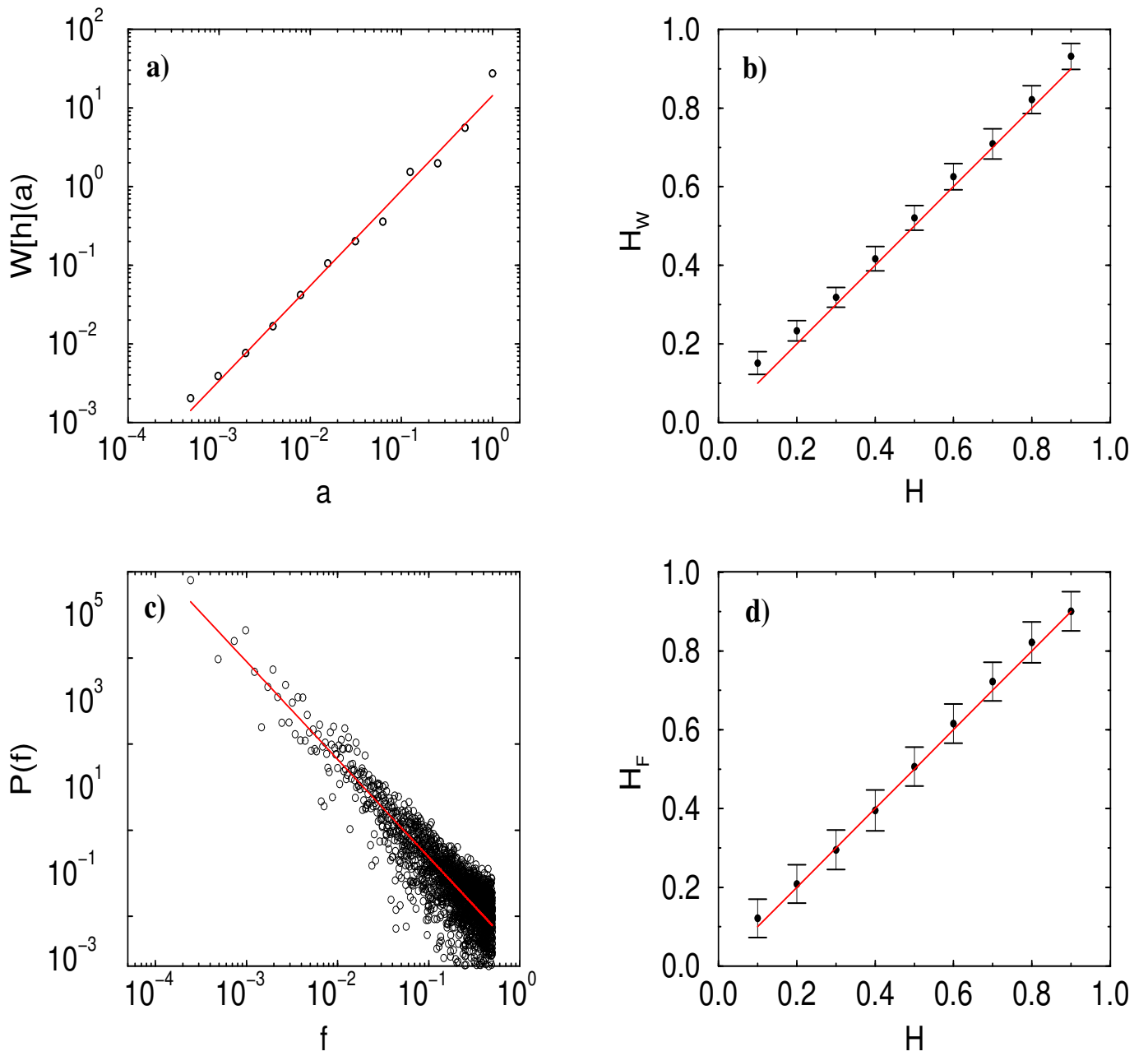


Figure 3

Simonsen, Hansen and Nes

Using the Wavelet transform for Hurst exponent determination

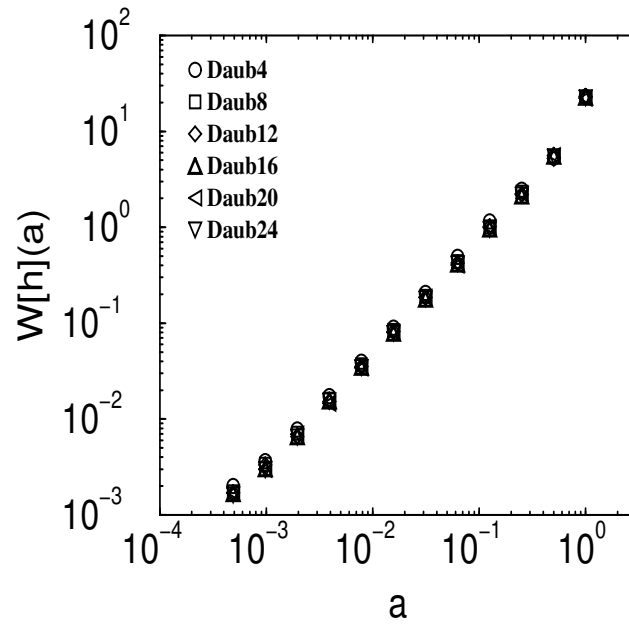


Figure 4

Simonsen, Hansen and Nes

Using the Wavelet transform for Hurst exponent determination

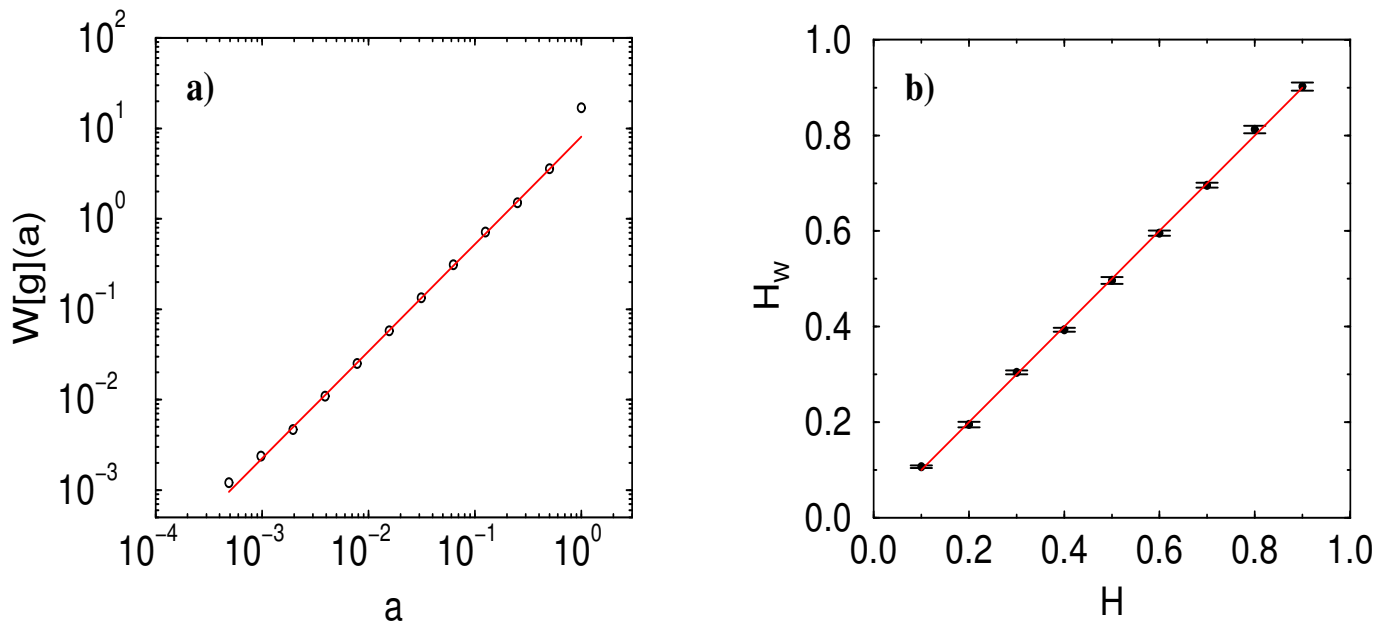


Figure 5

Simonsen, Hansen and Nes

Using the Wavelet transform for Hurst exponent determination

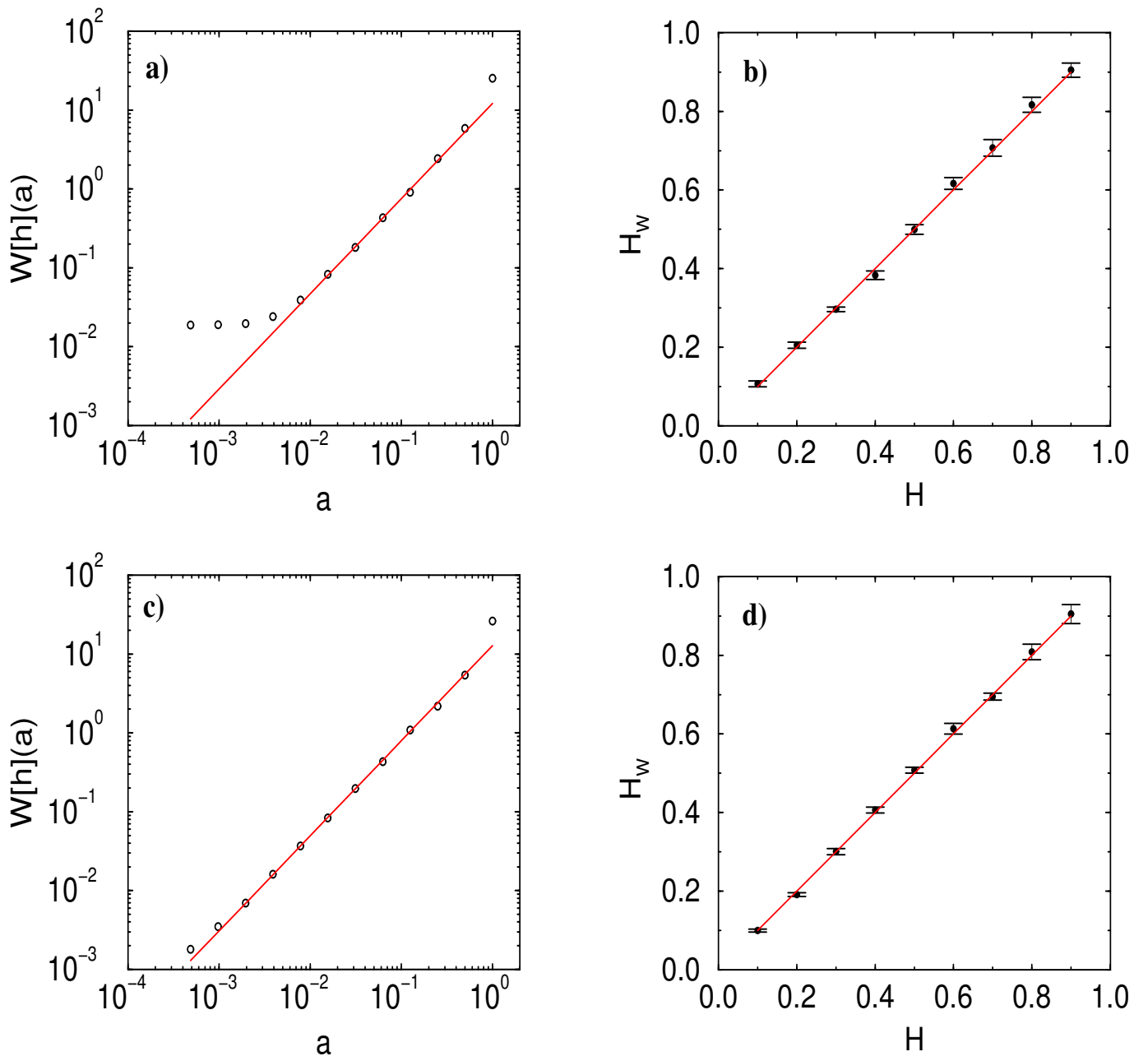


Figure 6

Simonsen, Hansen and Nes

Using the Wavelet transform for Hurst exponent determination

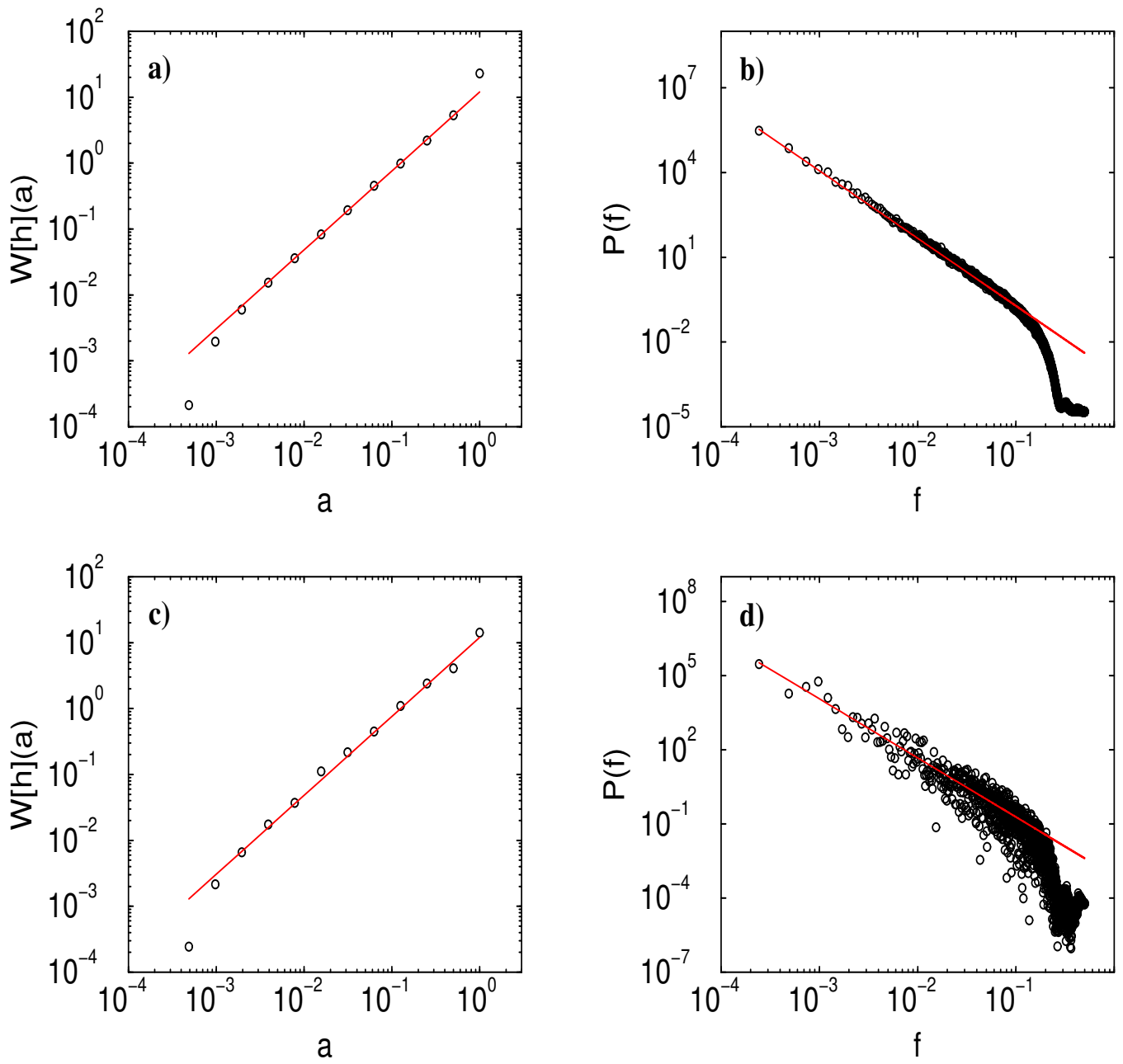


Figure 7

Simonsen, Hansen and Nes

Using the Wavelet transform for Hurst exponent determination

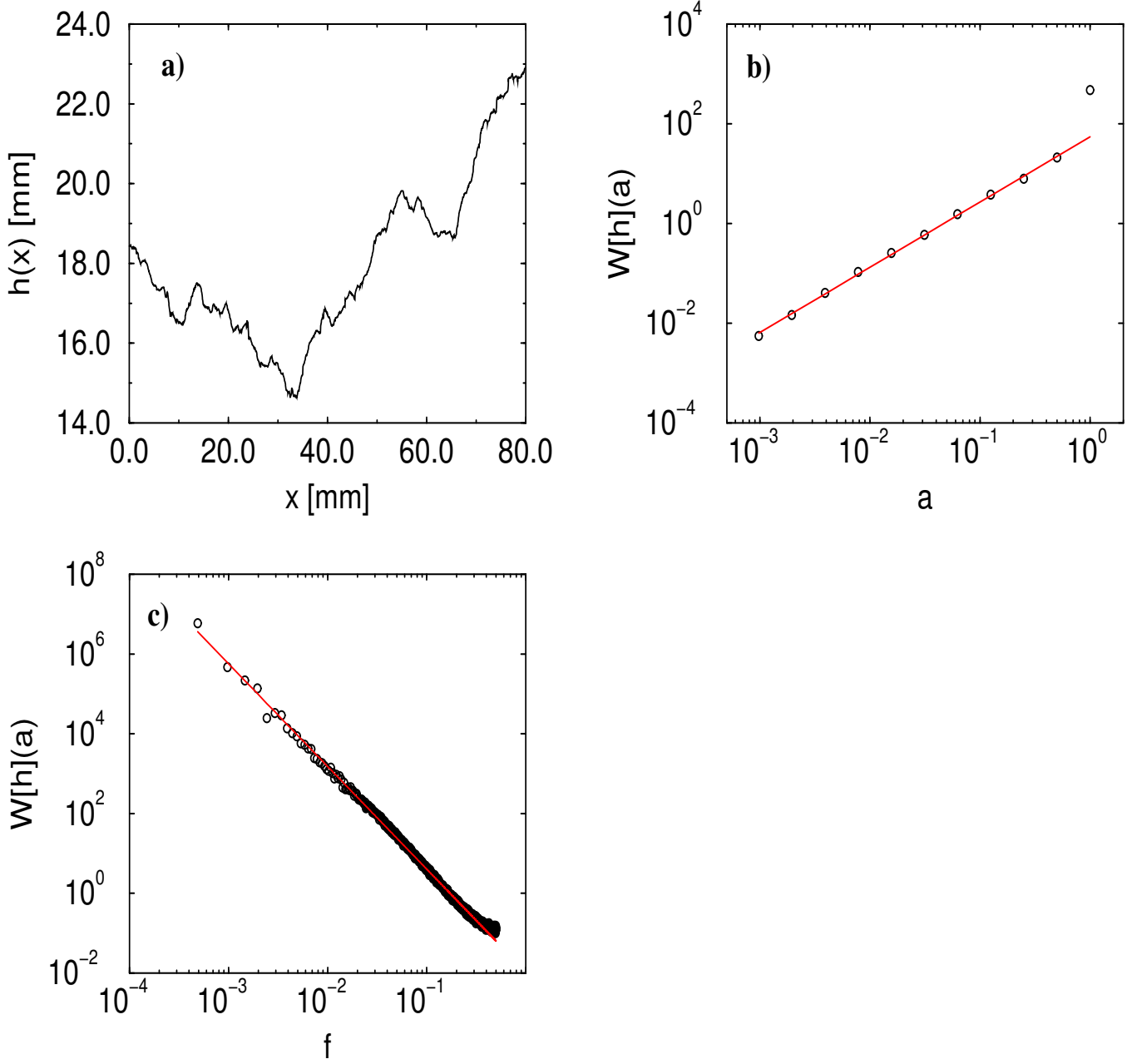


Figure 8

Simonsen, Hansen and Nes

Using the Wavelet transform for Hurst exponent determination

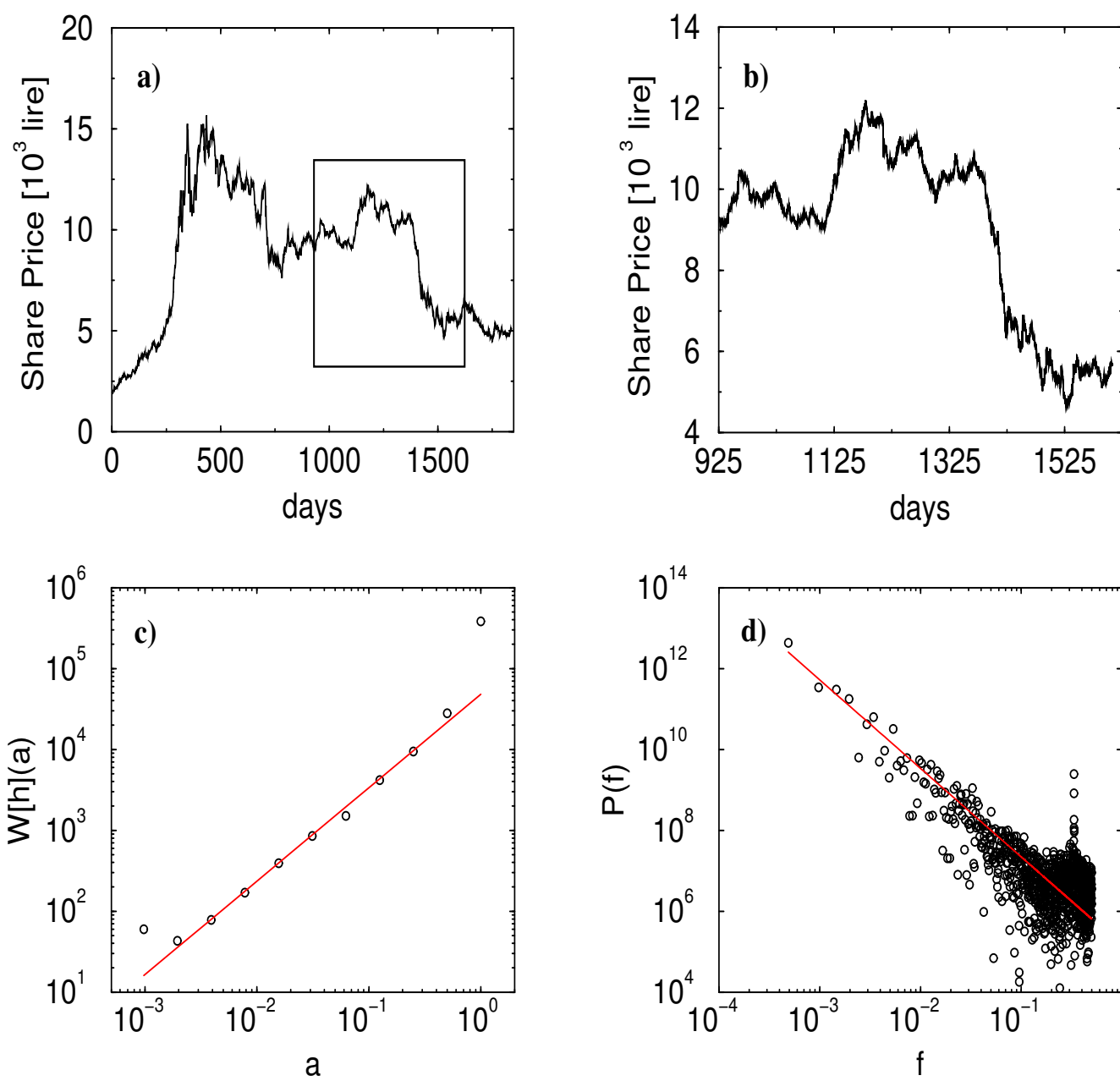


Figure 9

Simonsen, Hansen and Nes

Using the Wavelet transform for Hurst exponent determination